Arabian Journal of Chemistry (2022) **15**, 103900

King Saud University

Arabian Journal of Chemistry

www.ksu.edu.sa
www.sciencedirect.com

ORIGINAL ARTICLE

UV/TiO_2 photodegradation of metronidazole, ciprofloxacin and sulfamethoxazole in aqueous solution: An optimization and kinetic study

Surya Akter [a,b], Md. Shahinoor Islam [c], Md. Humayun Kabir [a], Md. Aftab Ali Shaikh [a], Md. Abdul Gafur [a,*]

[a] *Bangladesh Council of Scientific and Industrial Research (BCSIR), Dhaka, Bangladesh*
[b] *Department of Materials and Metallurgical Engineering, Bangladesh University of Engineering & Technology, Dhaka, Bangladesh*
[c] *Department of Chemical Engineering, Bangladesh University of Engineering & Technology, Dhaka, Bangladesh*

Received 8 December 2021; accepted 3 April 2022
Available online 12 April 2022

KEYWORDS

Ciprofloxacin;
Degradation kinetics;
Metronidazole;
Sulfamethoxazole;
Photodegradation

Abstract Emerging pharmaceutical ingredients (APIs) like sulfamethoxazole (SMX), metronidazole (MNZ) and ciprofloxacin (CIP) are biopersistent and toxic to the environment and public health. In this study, UV/TiO_2 photodegradation was applied in the degradation of SMX, MNZ and CIP individually and in a mixture. For a 5 mg/L SMX solution, about 97% of SMX was degraded within 360 min, which was reduced to 80% for 80 mg/L of SMX solution at the same TiO_2 dosage and photodegradation time. The maximum removals of MNZ and CIP as individual components were 100% and 89%, respectively at 600 min of photodegradation reaction time. For binary mixtures, the highest removal (100%) was achieved for MNZ and CIP ([MNZ] = [CIP] = 40 mg/L) mixture at 120 min whereas the degradations were 97% and 96% for SMX and MNZ, and SMX and CIP binary mixtures, respectively, even after 600 min of experimental time at the same concentrations. For tertiary mixture, the maximum degradation 99% was observed for (SMX = CIP] = 20 mg/L and [MNZ] = [40 mg/L) at 600 min. The observed reaction rate was 0.01085 min^{-1} when SMX concentration was 5 mg/L, which decreased to 0.00501 min^{-1} for SMX concentration of 80 mg/L, indicating decreasing of reaction rate at higher concentration.

Abbreviations: SMX, Sulfamethoxazole; MNZ, Metronidazole; CIP, Ciprofloxacin; AOP, Advanced oxidization process; LC-MS, Liquid chromatography mass spectrometry

* Corresponding author at: Principal Scientific Officer, BCSIR, Dhaka, Bangladesh.
E-mail addresses: ripasurya@gmail.com (S. Akter), shahinoorislam@che.buet.ac.bd (M.S. Islam), h.kabir79@yahoo.com (M.H. Kabir), aftab74@yahoo.com (Md. Aftab Ali Shaikh), dr.abdul.gafur.bcsir@gmail.com (M.A. Gafur).

Peer review under responsibility of King Saud University.

Production and hosting by Elsevier

https://doi.org/10.1016/j.arabjc.2022.103900

The results indicate that the UV/TiO_2 process is promising to apply for the treatment of pharmaceutical wastewaters.

1. Introduction

The industrial revolution is a blessing for human beings but the misuse and abuse of active pharmaceuticals ingredients, fertilizer, textile and industrial dye in the environment have accelerated the growing pollutants like diethyl phthalate, dimethyl phthalate, 2-4 dinitrophenol, etc. (Ahmadi et al., 2016; Azari et al., 2021a, 2021b, 2020; Yousefzadeh et al., 2017). Recently, the use of drugs has increased dramatically because of the spreading of various diseases (Kanakaraju et al., 2018). Thousands of different APIs (active pharmaceutical ingredients) are currently in use to treat or prevent human and animal diseases. In addition, APIs are extensively used as feed additives for livestock to promote the growth of animals (Carlsson et al., 2006). With the inadequate disposal of expired antibiotics and incomplete metabolism in the human and animal bodies, the concentration of antibiotics is increased in wastewaters day by day (Grenni et al., 2018; Malakootian and Ahmadian, 2019). Groundwater, surface water and river water are getting polluted by these drugs, which consequently affects the whole ecosystem of the contaminated region. For instance, Yantze river region, Guangzhon and Nairobi/Athi river basins (Kenya, East Africa) are regarded as contaminated hot spots from pharmaceutical ingredients (Bagnis et al., 2020; Leung et al., 2013). Among the different APIs, antibiotics are the main concern because of their biopersistent, toxic, carcinogenic and mutagenic nature (Gutierrez et al., 2013). The concentration of antibiotics in the surface waters is increasing day by day due to uncontrolled release and lack of proper treatment of hospital and municipal wastewaters before discharging. This causes multi-resistant bacteria to pose serious risks to human and veterinary health (Grenni et al., 2018). Antibiotics removal from wastewater is a great attraction for researchers due to their negative effects on various organisms and ecosystems. An effective treatment scheme for hospital and household wastewaters is urgently required for controlling the drug's concentration in the surface water bodies.

Hospital effluents contain 2–150 times higher concentrations of various drugs than in urban wastewater reported by Verlicch et al. (Verlicchi et al., 2010). Some antibiotics, like penicillin, are easily biodegraded, whereas others, like fluoroquinolones (e.g., ciprofloxacin), nitroimidazole (e.g., metronidazole), macrolides and tetracyclines, are significantly persistent. This leads to their remaining for an extended period in the environment, spreading wider and accumulating in higher concentrations. The input and presence of antibiotics and their fate in the environment are still of high interest because antibiotics pollution in rivers worldwide exceeds environmental safety thresholds (Khan et al., 2020). Metronidazole (MNZ, $C_6H_9N_3O_3$) is an imidazole antibiotic used for bacterial vaginosis and pelvic inflammatory disease (Neghi et al., 2019), ciprofloxacin (CIP, $C_{17}H_{18}N_3O_3F$) is a fluoroquinolone antibiotic mainly used for bacterial infections (Li et al., 2020), and sulfamethoxazole (SMX, $C_{10}H_{11}N_3O_3S$) is a sulfonamide antibiotic used for bronchitis and urinary tract infections (Xekoukoulotakis et al., 2011). They are widely used in both human and veterinary medicine and detected in aquatic environments like drinking water, ground/ surface water, soil sediments and wastewater from one to several ng L^{-1} (Neghi et al., 2019).

Recently, CIP, MNZ and SMX are shown as the most emerging pharmaceutical contaminants in Bangladesh. Anwar Hossain et al. found that the concentration of MNZ and SMX were distinctively higher in surface water of Bangladesh among nine APIs detected (Hossain et al., 2018; Hossain et al., 2017). Another study found that CIP is the highest concentration of antibiotics in Dhaka, Matlab sites and Rampura canal, Bangladesh. Susceptibility for select ESBL-p E. coli strains were tested and the study found that 85% of the strains were susceptible to CIP (Angeles et al., 2020). The bio persistent CIP, MNZ and SMX are almost ubiquitous in not only in surface water of Bangladesh but also globally.

Due to the potential adverse effects of antibiotics on human health, reliable techniques with stable removal effectiveness are highly desirable. Several treatment techniques including physical (e.g., membrane separation and adsorption) (Garcia-Ivars et al., 2017; Mahmoodi Meimand et al., 2019), chemical (Crini and Lichtfouse, 2019), biological (Martini et al., 2018) and advanced oxidization processes (AOPs) have been applied for the removal of antibiotics from water (Martini et al., 2018). Membrane separation and adsorption processes are not always effective to attain the discharge limits and are costly (Van der Bruggen et al., 2008). Chemical processes such as chlorination and ozonation produce secondary pollutants (halogenated byproducts) (Xu et al., 2002). Biological treatment cannot remove antibiotics completely from the water because of their toxic and biopersistent nature (Martini et al., 2018). AOPs including photo-Fenton, solar-photocatalytic and UV-based photocatalytic processes are promising techniques as a group of strong oxidizing agents such as superoxide radicals, peroxide radicals, persulfate radicals and hydroxyl radicals can be generated (Chen et al., 2021; Dharwadkar et al., 2021; Javid et al., 2020; Wu et al., 2020). These species are highly reactive and can degrade both biodegradable and nonbiodegradable organic pollutants from water (Shuchi et al., 2021; Tran et al., 2019). Recently, UV-based photocatalytic nanoparticles (NPs) have earned more attention to removing antibiotics from wastewater because it has the advantages of energy-saving without generating any secondary pollutants (Malakootian et al., 2020d, 2020a). Among the photocatalysts, TiO_2 NPs are widely used in the treatment of organics in water because of their high photoactivity, high chemical stability, low cost, nontoxic, narrow bandgap, reusable and applicable for a wide range of pH (Al-Mamun et al., 2021).

However, most of the UV-based TiO_2 photocatalysis process has been applied for a single compound. Individual studies of SMX, MNZ and CIP degradation have shown excellent performance (Farzadkia et al., 2015; Malakootian et al., 2019; Porcar-Santos et al., 2020; Silva et al., 2016). Impacts of operating parameters such pH, recirculatory flow, concentrations, catalyst dosage, UV light intensity and degradation kinetics have been studied well (Farzadkia et al., 2015; Salma et al., 2016). Competitive degradation of antibiotics in a mixture using photo- Fenton process (Perini et al., 2018) (mixture: ciprofloxacin, amoxicillin, sulfathiazole and sulfamethazine), solar simulator based Cu-modified TiO_2 (Evgenidou et al., 2021) (mixture: isoniazid, metronidazole, sulfadiazine, sulfamethoxazole, trimethoprim, norfloxacin, moxifloxacin and lincomycin) and UV based TiO_2 (metronidazole and amoxicillin) (Tran et al., 2019) process have been studied. Eleni Evgenidou et al used Pyrex glass reactor to remove a mixture of eight antibiotics and finally centrifuged to remove photocatalyst (0.8$CuTiO_2$) (Evgenidou et al., 2021). To our best knowledge, no study proposed the degradation of SMX, MNZ and CIP in a mixture using UV-based TiO_2 photocatalyst. In this context, the current study focused on UV-based TiO_2 photocatalytic degradation of SMX, MNZ and CIP antibiotics individually and in mixtures, with various combinations to understand the degradation behaviors and reaction kinetics.

TiO_2 can be applied through immobilization on glass and steel surfaces (Al-Mamun et al., 2021) or in an suspension in a photocatalytic reactor (Hasan Khan Neon and Islam, 2019). The photocatalytic activity of immobilized TiO_2 NPs was decreased whether the activity was remain unchanged after five cycle experiments for suspended experiments (Farzadkia et al., 2015). Suspended TiO_2 was settled from UV- TiO_2 treated solutions after 24 h settling to avoid centrifugation for large scale

applications. Therefore, the current study was carried out to investigate the photocatalytic performance of TiO_2 NPs in aquatic suspension in the treatment of SMX, MNZ and CIP antibiotics under UV-irradiation. The major objectives of the study were: optimization of TiO_2 NPs dosage, assessment of comparative degradations of SMX, MNZ and CIP antibiotics, study of degradation kinetics and assessment of competitive degradation of SMX, MNZ and CIP antibiotics in mixtures.

2. Materials and methods

2.1. Materials

The pharmaceutical metronidazole (MNZ), ciprofloxacin (CIP) and sulfamethoxazole (SMX) were obtained from Sigma-Aldrich, Chemie GmbH, Kappelwegl, Gemrany. TiO_2 (anatase, 99.9%, 25 nm) was collected from Inframet Advanced Materials, USA, product# 22 N-0803A, Lot# TiO_2-N9140A3. Deionized water was collected from an ISO LAB (INARS, BCSIR, Dhaka, Bangladesh) and was used to prepare all stock solutions of antibiotics and used for dilutions for LC-MS analysis. The Nylon membrane 0.22 υm, 25 mm; PTFE; chrodisc by CHM was used for filtering the samples during the degradation. Formic acid, 98–100%, EssentQ® (Scharlau, Sentmenat, Spain) and acetonitrile, LC-MS (Scharlau, Sentmenat, Spain) were used for LC-MS analysis. Methanol and ethanol were purchased from Merck (HPLC grade, Germany). Ethanol was used for cleaning purpose and methanol was used as solvent to make standard sample for LC-MS analysis. All chemicals were used without any further purification. An Orbital sharer (JSOS-300, JSR, Rep. of Korea) was used for mixing purpose of all solutions.

2.2. Characterization of TiO_2 NPs

The powder X-ray diffraction (XRD) patterns were done using D8 Advance, Bruker AXS, Germany XRD with Cu Kα radiation (λ = 1.5418 Å) at a scan rate of 2° min^{-1} from 10° to 90° following 40 kV of accelerating voltage and 40 mA of applied current.

2.3. Photocatalytic experiment

A simple photocatalytic reactor was used for the degradation of antibiotics and the schematic of the experimental set-up is shown in Fig. 1. Three (3) ultraviolet light, 8 W of each (254 nm) was used for the UV-irradiation source and a minimum distance (4.5 cm) was maintained between photocatalyst and radiation source so that the maximum fraction of UV light is utilized to generate a large number of hydroxyl radicals. All photodegradation experiments were performed in the same photoreactor so that it is easy to make an authentic comparison of the results.

A stock solution of SMX (80 mg/L) was prepared and stored in a refrigerator at 4 ^{0}C. To study the impact of TiO_2 dosage on SMX under UV-irradiation, different concentrations of TiO_2 were added in a predetermined volume of prepared SMX solution and stirred at 250 rpm. Experiments were carried out for selected TiO_2 dosages of 0.5 g/L, 0.7 g/L and 1 g/L at room temperature for 6 h. The optimum dosage was determined based on SMX removal (0.7 g/L), and this optimum dosage was used for further studies. The impact of SMX concentration on UV-irradiation/TiO_2 process performance was evaluated by changing SMX concentrations ranging from 5 to 80 mg/L. Then stock solutions for three antibiotics - metronidazole (MNZ), ciprofloxacin (CIP) and sulfamethoxazole (SMX) were prepared to study global degradation of MNZ, CIP and SMX mixtures. All stock solutions were kept in a refrigerator (at 4 ^{0}C) before use and all solutions are used at their inherent pH (MNZ = 6.54, SMX = 5.4 and CIP = 6.04) and without controlling temperature.

Before performing the photocatalytic experiment, an adsorption control experiment of TiO_2 was performed under dark conditions. The solution loaded with TiO_2 was stirred under dark for 60 min and a 5 mL solution was withdrawn using a syringe at distinct time intervals. The solutions were kept 24 h to settle down the suspended TiO_2 Nps from solutions. The samples were then analyzed after filtration using a nylon membrane filter (pore size: 0.22 μm, dia: 25 mm; PTFE; chrodisc by CHM). The UV–vis absorption spectra of MNZ, CIP and SMX were measured using a UH4150 Spectrophotometer (PerkinElmer).

2.4. LC-MS/MS analysis

The LC-MS/MS instrument was of Agilent 6420 LC and TQ 1290, USA. A ZORBAX Eclipse Plus C18 rapid resolution HD 2.1 × 100 mm column, USA 1.8 μm was used for online extraction. The mobile phases consisted of A: 0.1% formic acid and B: 15% acetonitrile. Mobile phase C was used for cleaning the columns after separation.The ionization chamber

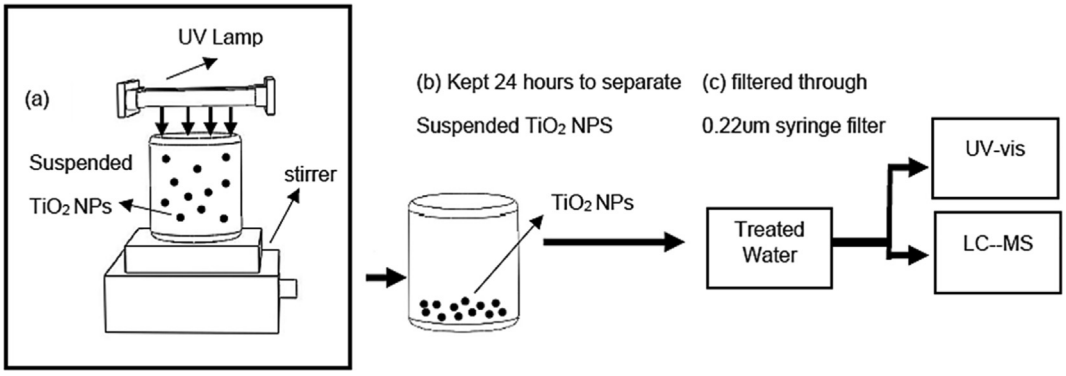

Fig. 1 Experimental set-up representation.

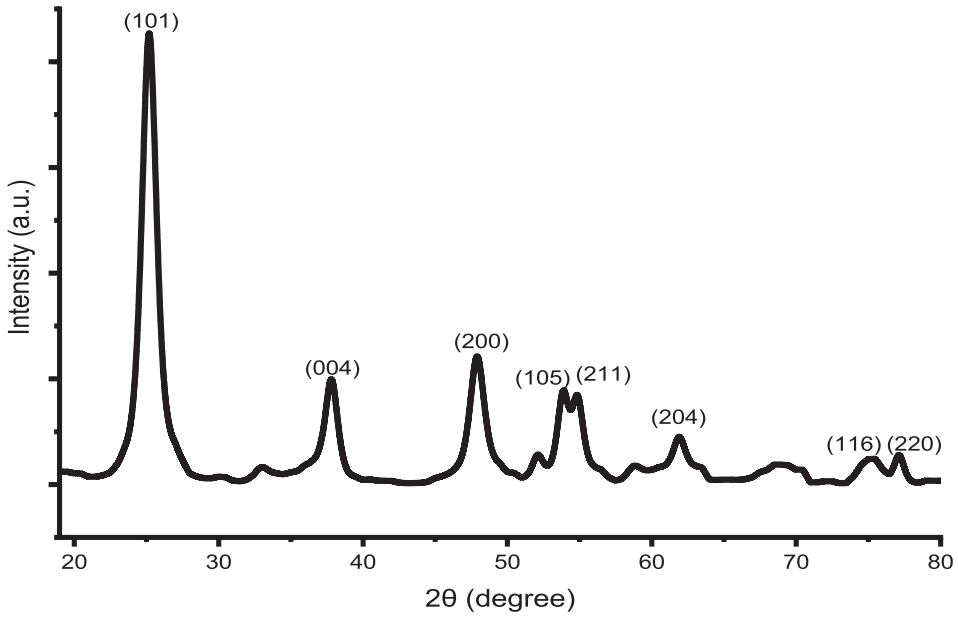

Fig. 2 XRD patterns of TiO2 nanoparticles.

was equipped with an electrospray ionization interface operated in positive-ion mode and the interface and total flow was 0.4 m/min. Quantification was performed using multiple reaction monitoring (MRM). MRM transitions, collision energies and dwell voltage fragmentor, and cell accelerator voltage are presented in Table S1. The whole LC-MS equipment was kept in a temperature-controlled environment at 27 °C. Samples were stored in the autosampler were kept at 4 °C before analysis and injected volume was 5 µl. The global degradation of the antibiotics was calculated from the initial and final area from the LC-MS analysis of three antibiotics.

2.5. Data analysis

The removal efficiency of antibiotics was calculated using the following equations:

$\%\,R = \frac{C0-Ct}{Co} \times 100\%$ (1) where C_0 and C_t are the initial and the residual concentrations of the antibiotics at t time (mg/L), respectively.

The degradation kinetics of antibiotics in a batch system was explained by zero-order, pseudo-first-order, and second-order kinetic models. The kinetic models by photocatalytic degradation of antibiotics are presented by Eqs. (2)–(4).

Zero-order kinetics:

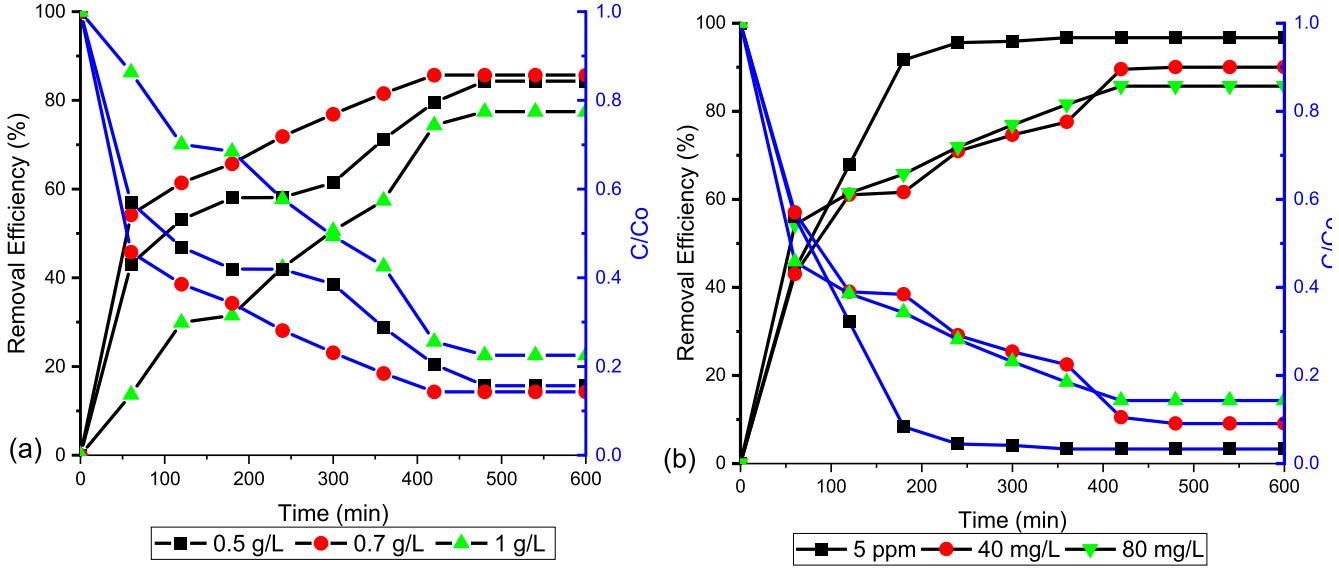

Fig. 3 The effect of catalyst dosage and initial SMX concentration on the photocatalytic degradation of SMX. a) effect of catalyst dosage for, [SMX] = 80 mg/L and b) effect of initial SMX concentration for TiO_2 = 0.7 g/L.

Table 1 Comparison of photocatalytic degradation of SMX, MNZ and CIP with the literature value.

Antibiotics	Systems	Catalyst dosage (g/L)	Initial concentration (mg/L)	UV-irradiation parameters	Time (min)	Removal efficiency (%)	Reference
SMX	UV/TiO_2	0.7	5	24 W λ = 254 nm Path length 4.5 cm	360	97%	Present study
	UV/TiO_2	0.7	40	24 W λ = 254 nm Path length 4.5 cm	480	92%	Present study
	UV/TiO_2	0.7	80	24 W λ = 254 nm Path length 4.5 cm	480	86%	Present study
	UV/TiO_2 immobilized on glass plates	4	10	18 W λ = 254 nm	420	97%	(Ahmed and Zahraa, 2014)
	Xenon lamp/TiO_2	0.5	100	Xenon lamp (PHILIPS XOP-15-OF, 1000 W)	360	82%	(Abellán et al., 2007)
	UV/TiO2	0.2	10	50 W xenon lamp	180	58%	(Zhang et al., 2017)
	UV/TiO2/pBC	0.2	10	50 W xenon lamp	180	91%	(Zhang et al., 2017)
	UV/biochar/TiO2	0.5	10	15 W λ = 350 nm	180	75%	(Kim and Kan, 2016)
MNZ	UV/TiO_2	0.7	80	24 W λ = 254 nm Path length 4.5 cm	600	100%	Present study
	UV/ TiO_2	2.5	0.1	32 W λ = 254 nm	120	100%	(N and Kumar, 2017)
	UV/TiO_2	2.5	100	32 W λ = 254 nm	120	47%	(N and Kumar, 2017)
	UV/polymeric-TiO_2	0.3	0.1	32 W λ = 254 nm	120	34%	(Neghi et al., 2019)
	UV/polymeric-TiO_2	0.3	10	32 W λ = 254 nm	120	18%	(Neghi et al., 2019)
	UV/TiO_2	0.5	80	125 W λ = 254 nm	120	99%	(Farzadkia et al., 2015)
CIP.	UV/TiO_2	0.7	80	24 W λ = 254 nm Path length 4.5 cm	600	89%	Present study
	UV/TiO_2 immobilized on glass plates	0.12	20	Irradiance 100Wm-^{2} λ = 365 nm	480	75%	(Triquet et al., 2020)
	UV/TiO_2	0.12	20	Irradiance 100 Wm-^{2} λ = 365 nm	60	75%	(Triquet et al., 2020)
	UV/GMC-TiO2 composite	0.35	15	14 W λ = 254 nm	90	100%	(Zheng et al., 2018)
	UV/TiO_2 immobilized on glass plates	1	3	6 W λ = 254 nm	105	92%	(Malakootian et al., 2020c, p. 2)
	Xenon lamp/TiO2 (hydrothermal)	0.25	160	500 W Xenon lamp (CEL-LAX500)	360	96%	(Gan et al., 2018)

$$C_t - C_o = k_o t \quad (3)$$

First-order kinetics:

$$\ln\left(\frac{C_o}{C_t}\right) = k_1 t \quad (4)$$

Second-order kinetics:

$$\frac{1}{C_t} - \frac{1}{C_o} = k_2 t \quad (5)$$

where k_0 (mg/L-min), k_1 (1/min), and k_2 (L/mg-min), represent the apparent kinetic rate constants of zero, pseudo-first and second-order reaction kinetics, respectively.

3. Results and discussion

3.1. Characterization of TiO_2

Fig. 2 shows the crystal phases of TiO_2 nanoparticles using XRD analysis. The results matched with JCPDS 96-900-

8217. The diffraction peaks occurring at 25.156°, 37.385°, 47.782°, 53.344°, 54.753°, 62.191, 68.052, 69.884 and 74.397° have been assigned to the (101), (004), (200), (105), (211), (204), (116), (220) and (215) lattice planes of pure tetragonal anatase phase of TiO_2, respectively.

3.2. Photocatalytic activity analyses

3.2.1. Photodegradation analyses of SMX

Fig. 3a shows the percentage of removal efficiency and relative concentration (C/Co) of SMX with UV irradiation time for different doses of TiO_2. The SMX removal efficiency was increased with UV irradiation time, whereas the relative concentration of SMX was decreased. The initial rate of SMX degradation was high, however, the degradation rate was decreased with experimental time increase. The figure also reveals the impact of photocatalyst TiO_2 dosage on SMX degradation. For a 0.5 g/L TiO_2 dosage in the reactor, the removal efficiency was 43% at 60 min of UV irradiation time and it increased to 53% for 0.7 g/L TiO_2. The removal efficiency increased with increasing catalyst dosage because a large number of active sites were provided, which promoted the generation of hydroxyl radical and enhanced the degradation of SMX. Thus, the maximum removal efficiency reached 97 % for the 0.7 g/L TiO_2 dosages (C/Co reached 0.1429) after 420 min of UV irradiation time. However, with further addition of TiO_2 (1 g/L), the removal decreased to 14% at 60 min indicating an overdose of catalyst scavenged hydroxyl radicals (•OH) and inhibited the degradation of antibiotics (Wang and Zhuan, 2020). Excessive catalyst dosage would block incident UV light (Wang et al., 2010, 2012) and cause the loss of light energy through shielding, reflection and scattering of light by solid particles (Mourid et al., 2020). Therefore, the optimum catalyst dosage of 0.7 g/L TiO_2 was selected for the rest of the studies to be carried out. Fig. 3b shows the effect of different concentrations of SMX on the photoreactor performance for the optimum dosage (0.7 g/L TiO_2). SMX concentrations were varied for 5 mg/L, 40 mg/L and 80 mg/L. The figure represents the removal efficiency decreased with concentrations increased. Maximum 97%, 88% and 82% removal efficiencies were achieved within 480 min for 5 mg/L, 40 mg/L and 80 mg/L SMX, respectively. The degradation rate was 92% for 5 mg/L against 65% for 80 mg/L of SMX concentration (Fig. 3b) after 180 min indicating that antibiotic concentration has a great impact on degradation using UV/TiO_2 process. Fig. S1 shows the evolution of the UV–vis absorption spectrum of SMX (5 mg/L) depending on the irradiation time. The top curve is for the initial time and SMX has a maximum absorbance peak at 270 nm. With the irradiation time, the intensity of the peak decreased and finally, it became flat after 360 min of experimental time, indicating the degradation of SMX under UV/TiO_2 photocatalysis.

UV-irradiation parameters, catalyst dosage and removal efficiencies of SMX, MNZ and CIP are summarized in Table 1. Previously, Ahmed et al. (Ahmed and Zahraa, 2014) and Abellán et al. (Abellán et al., 2007) used TiO_2 as a photocatalyst to degrade SMX. According to Ahmed et al. and Abellán et al, the maximum removal efficiencies were 97% and 82% after 420 min (for 10 ppm) and 360 min (for 100 ppm) of UV irradiation time, respectively (Table 1). Their UV irradiation parameters are given in Table 1. Ahmed et al. (Ahmed and Zahraa, 2014) used TiO_2 immobilized glass plate (4 g/L TiO_2) in their study under UV-irradiation with 18 W lamp. A lower dosage (0.5 g/L TiO_2) was applied in a suspended system (Abellán et al., 2007) but removal efficiency was lower than the present study as they used a higher concentration of SMX (100 ppm).

3.2.2. Photodegradation analyses of MNZ and CIP

Photocatalytic degradation of MNZ (80 mg/L) was carried out using optimum TiO_2 dosage (0.7 g/L) and the results are shown in Table 1 and Fig. 4. Fig. 4a depicts that as irradiation time increased, the percentage removal efficiency of MNZ increased. After 60 min of experimental time, the MNZ degradation was only 16% which reached 81% at 360 min and 100% at 600 min of experimental time. The C/Co tends to zero as observed in Fig. 4a. Similar results were found by other researchers (Neghi and Kumar, 2017). N and Kumar, (2017) applied 2.5 g/L TiO_2 dosage for different concentrations of MNZ, and the study revealed that (Neghi and Kumar, 2017) 100% removal of MNZ was observed for low concentration (0.1 mg/L MNZ) after 120 min, which decreased to 47% (max-

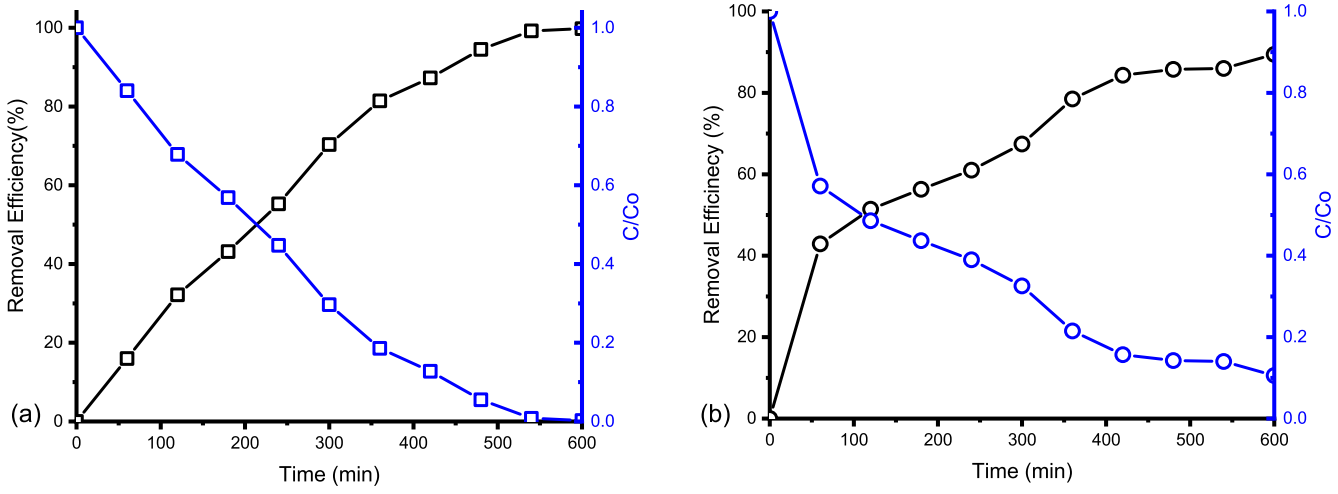

Fig. 4 Photocatalytic degradations of MNZ and CIP for 80 mg/L using TiO2 of 0.7 g/L. a); percentage removal of MNZ concentration and b) percentage removal of CIP concentration.

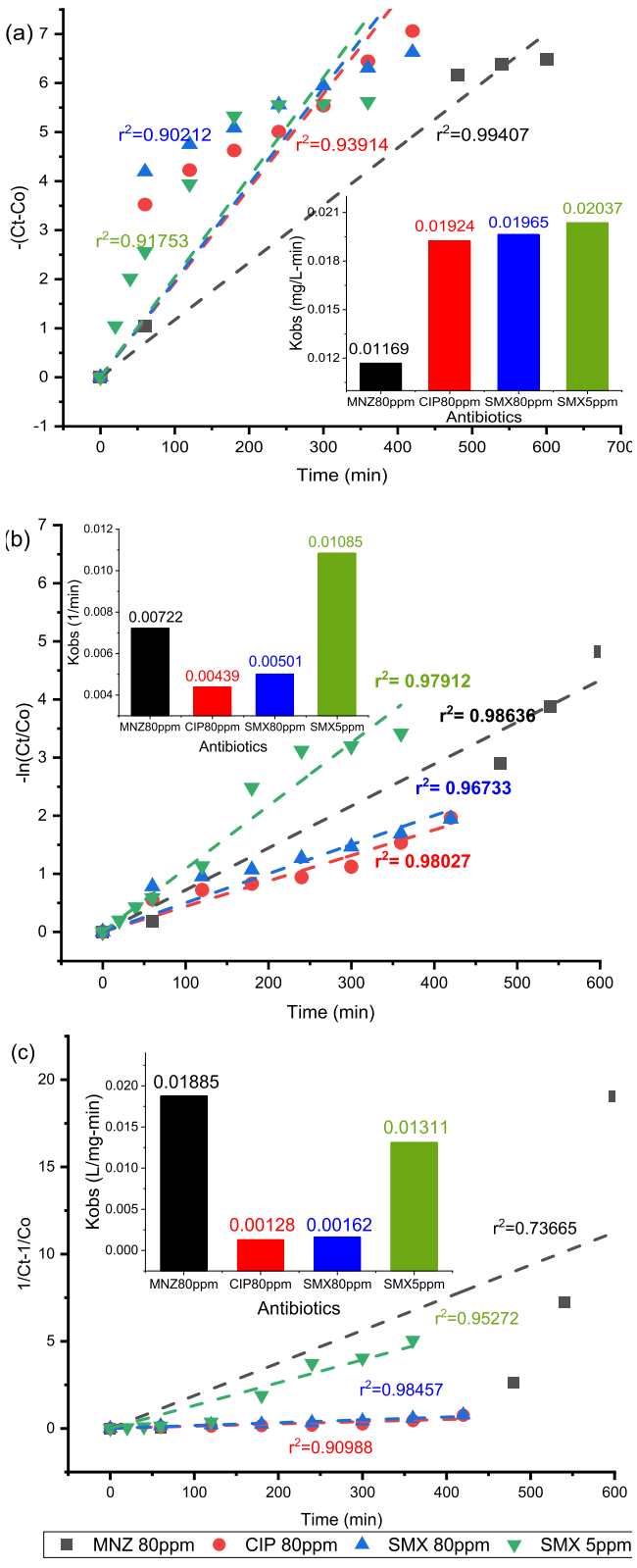

Fig. 5 Kinetics curves of MNZ, CIP and SMX (TiO_2 = 0.7 g/L) (a) zero order, (b) 1st order and (c) 2nd order; inset: Kinetic parameters of different condition.

imum) for a higher concentration (100 mg/L) of MNZ. Neghi et al. (2019) applied lower photocatalyst dosage (0.3 g/L) for the the degradation of 10 mg/L MNZ solution and observed 18% degradation after 120 min indicating lower dosage was not effective for the removal of MNZ for a short period experiment. Fig. S2 shows the evolution of the UV–vis absorption spectrum of MNZ with irradiation time. The top curve represents the spectrum for the initial concentration of MNZ (80 mg/L) has a maximum peak intensity at 314 nm. The peak intensity of MNZ was decreased with time. After 600 min of experimental time, the peak intensity became flat indicating near 100% removal of MNZ.

Fig. 4b shows photocatalytic degradation (percentages removal and relative concentration) of CIP (80 mg/L) using the optimum TiO_2 dosage of 0.7 g/L. A similar degradation trend was observed as obtained for SMX and MNZ degradations. The figure indicates that the removal efficiency increased with irradiation time. After 60 min of the experiment, the degradation was 43%, which increased to 78% at 360 min and 89% at 600 min. Very similar results were obtained by Triquet et al. (2020). Triquet et al. (2020) applied (TiO_2 0.12 g/L) suspended TiO_2 and coated TiO_2 on the glass plate for the degradation of 20 mg/L CIP and the observed rate constant was higher for suspended TiO_2. 75% CIP removal was observed for immobilized and suapended system after 480 min and 60 min, respectively. However, considering the separation of expensive TiO_2 for a suspension system, TiO_2 immobilized on glass plates system was considered as a promising technique. Fig. S3 shows the evolution of the UV–vis absorption spectrum of CIP degradation depending on the irradiation time. The top curve is for the initial concentration of CIP which has a maximum absorbance at 272 nm. With the passage of the experimental time, the absorbances peak was decreased.

3.3. Reaction kinetics study

Kinetic study is important to understand the degradation rate and design of a photocatalytic reactor. Fig. 5(a), (b) and (c) shows the zero order, 1st order and 2nd order kinetic curves of SMX (5&80 ppm), MNZ and CIP (80 ppm). The kinetics data of MNZ, SMX and CIP fitted best to the pseudo 1st order.The kinetics curve of SMX for 5 and 80 mg/L and MNZ and CIP for 80 mg/L for 0.7 g/L TiO_2. The figure illustrates that the slope of 5 mg/L SMX is higher than the slope of 80 mg/L SMX, CIP and MNZ. To evaluate photocatalytic activity of TiO_2 for MNZ, CIP and SMX observed rate constant (min^{-1}) (K_{obs}) was calculated from the slope of -ln(C/Co) vs time curve. Fig. 5(b) shows the values of calculated rate constants for MNZ, CIP and SMX. The rate constants were 0.01085 min^{-1} and 0.00501 min^{-1} for 5 mg/L and 80 mg/L of SMX, respectively. For a higher SMX concentration, active sites of TiO_2 were covered by the target molecule that retard the generation of the hydroxyl radicals (Ahmed and Zahraa, 2014; Xekoukoulotakis et al., 2011). Among SMX, MNZ and CIP, the reaction rate constant for MNZ was the highest. The lowest value of rate constant was observed for CIP.

3.4. Competitive degradation of MNZ, CIP and SMX

The evolution of the UV–vis absorption spectrum of mixture antibiotics is shown in Fig. S4. As shown in Fig. S4, the peaks of SMX and CIP were observed at same wavelength and there-

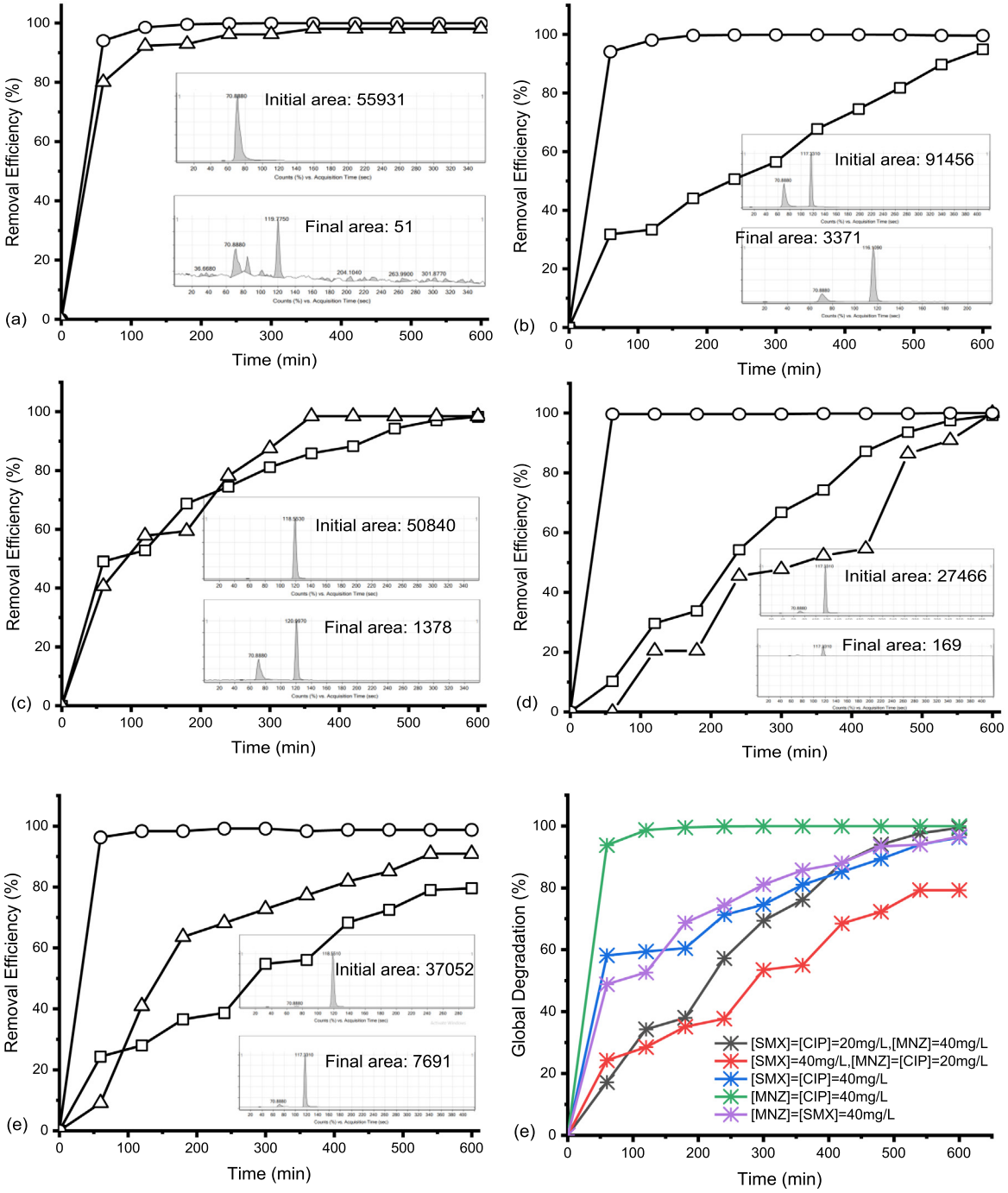

Fig. 6 Removal Efficiency vs time curve with LC-MS extracted ion chromatogram (a) [MNZ] = [CIP] = 40 mg/L, (b) [SMX] = [CIP] = 40 mg/L, (c) [SMX] = [MNZ] = 40 mg/L, (d) [MNZ] = 40 mg/L, [SMX] = [CIP] = 20 mg/L and (e) [SMX] = 40 mg/L, [MNZ] = [CIP] = 20 mg/L depending on the irradiation time (TiO_2 = 0.7 g/L). Symbols:(■) SMX; (●) CIP; (▲) MNZ. (f) Global degradation of CIP, SMX and MNZ. (In mixture condition; TiO2 = 0.7 g/L).

fore, it was difficult to identify the competitive degradation of SMX and CIP. Therefore LC-MS analysis was performed to understand the competitive degradation of SMX and CIP under UV-irradiation.

The LC-MS analysis results of degradation of SMX, MNZ and CIP are represented in Fig. 6. Fig. 6(a), (b), (c) and (d) shows the competitive degradation of [MNZ] = [CIP] = 40 mg/L, [SMX] = [CIP] = 40 mg/L, [SMX] = [MNZ] = 40 m g/L, [MNZ] = 40 mg/L, [SMX] = [CIP] = 20 mg/L and [SMX] = 40 mg/L, [MNZ] = [CIP] = 20 mg/L respectively with LC-MS extracted ion chromatogram. Before degradation, maximum peaks of SMX, MNZ and CIP were found at 117, 85 and 70, respectively. The decrease of area proves that photocatalytic degradation of antibiotics took place with UV irradi-

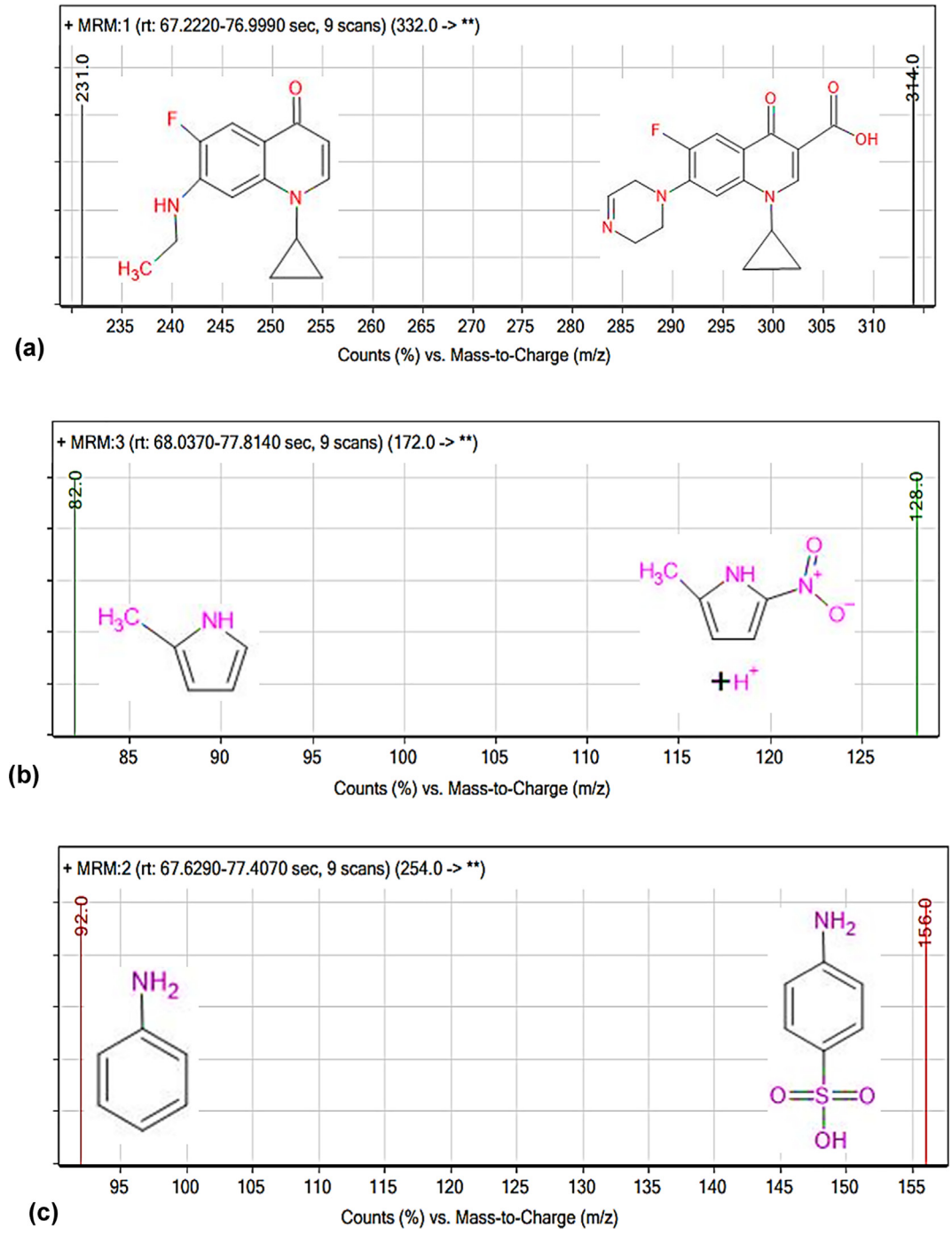

Fig. 7 LC-MS mass spectra of generated ions of (a)CIP, (b)MNZ and (c)SMX.

ation time. The mass spectra of SMX, MNZ and CIP are shown in Fig. 7. m/Z are 254 (Fig. 7(c)), 332 (Fig. 7(a)) and 172 (Fig. 7(b)) corresponding to the molecular weight [M + H] of CIP, MNZ and SMX. The product ions (Table S1) are related to the intermediate products which are formed during photodegradation.

Fig. 6a represents competitive degradation of [MNZ] = [CIP] = 40 mg/L. The photodegradation of both MNZ and CIP were faster and more than 90% of both MNZ (92%) and CIP (97%) were degraded within 120 min. The curve indicates CIP degradation was slight faster than MNZ antibiotics. In contrast, Fig. 6b indicates the degradation of SMX was slower than the degradation of CIP in a mixture of SMX and CIP ([SMX] = [CIP] = 40 mg/L). After 60 min, CIP and SMX degradations were 92% and 32% respectively, indicating the faster degradation of CIP as compared to SMX. Fig. 6c represents photodegradation results for SMX and MNZ mixture with a concentration of 40 mg/L for each antibiotics. The results indicate a very similar trend of degradation of both antibiotics when present at similar concentration ([SMX] = [MNZ] = 40 mg/L). Fig. 6d and 6e represents the degradation of tertiary mixtures of MNZ, SMX and CIP

Table 2 Comparison of global degradation of mixer antibiotics using LC-MS analysis.

Systems	pH	dosage (g/L)	$[Antibiotics]_0$ mg/L	Photodegradation parameter	Time (min)	Global deg. (%)	Reference
pistachio shell powder coated with ZnO NPs	5	1 g/L	[Tetracycline] = [Amoxicillin] = [Ciprofloxacin] = 60	adsorption	120	81%	(Mohammed et al., 2020)
Photo-Fenton UVC process	2.5	–	[Ciprofloxacin] = [Amoxicillin] = [Sulfathiazole] = [Sulfamethazine] = 0.2	30 W λ = 254 nm Path length1.5 cm	30	100%	(Perini et al., 2018)
UV/0.8CuTiO$_2$	–	0.1	[Isoniazid] = [Metronidazole] = [Sulfadiazine] = [Sulfamethoxazole] = [Trimethoprim] = [Norfloxacin] = [Moxifloxacin] = [Lincomycin] = 1	Irradiance 500 W m^{-2} λ > 300 nm	30	100%	(Evgenidou et al., 2021)
Solar Photocatalysis/TiO$_2$	7.5	0.5	[oxolinic acid] = [oxytetracycline] = 20	solar photocatalytic CPC reactor	30	100%	(Pereira et al., 2013, p. 2)
UV/TiO$_2$	7	1.5	[Metronidazole] = [Amoxicillin] = 50	100 W Irradiance 65 W m − 2 λ = 254 nm	120	70%	(Tran et al., 2019)
UV/TiO$_2$	–	0.7	[Metronidazole] = [Ciprofloxacin] = 40	24 W λ = 254 nm Path length 4.5 cm	120	100%	Present study
UV/TiO$_2$	–	0.7	[Sulfamethoxazole] = [Ciprofloxacin] = 20 [Metronidazole] = 40	24 W λ = 254 nm Path length 4.5 cm	600	99%	Present study
UV/TiO$_2$	–	0.7	[Sulfamethoxazole] [Metronidazole] = 40	24 W λ = 254 nm Path length 4.5 cm	600	97%	Present study
UV/TiO$_2$	–	0.7	[Sulfamethoxazole] = [Ciprofloxacin] = 40	24 W λ = 254 nm Path length 4.5 cm	600	96%	Present study
UV/TiO$_2$	–	0.7	[Sulfamethoxazole] = 40 [Metronidazole] = [Ciprofloxacin] = 20	24 W λ = 254 nm Path length 4.5 cm	540	79%	Present study

with concentrations [MNZ] = 40 mg/L, [SMX] = [CIP] = 20 mg/Land [SMX] = 40 mg/L, [MNZ] = [CIP] = 20 mg/L , respectively. As shown in Fig. 6d, the degradation trend was CIP > SMX > MNZ, which might be a reason of using higher concentration of MNZ in reaction mixture. The degradation trend in Fig. 6e was CIP > MNZ > SMX justified the use of higher concentration of SMX in the mixture.

Table 2 represents the LC-MS results for mixture of antibiotics. From Table 2 it can be concluded that 100% efficiency can be achieved within 30 min (Evgenidou et al., 2021; Perini et al., 2018), when the concentration of mixer of 8 antibiotics was 1 mg/L each for 0.1 g/L of Cu-TiO$_2$ composite under 500 W UV light. In the current study, the maximum antibiotics degradation efficiency is 100% for an irradiation time of 120 min for [MNZ] = [CIP] = 40 mg/L. The degradation time is higher than that obtained in previous studies as we used a higher concentration of mixer antibiotics. Joao A. et al used the photo-Fenton UVC process (Perini et al., 2018). Due to the formation of solid sludge, as iron ions continuously lose during this process, Fenton has some economic and environmental drawbacks (Babuponnusami and Muthukumar, 2014). For the mixture of SMX, MNZ, CIP, 99% removal efficiency was achieved at 600 min and removal efficiency decreased to 79% when concentration for SMX was higher. The probable reason is the formation of 4-amino-N-(5-methyl-2-oxazolyl) benzenesulfonamide during photodegradation, which is an isomer of SMX (Fig. 8(a)). In contrast in the case of MNZ and CIP, unstable products, hydroxyethyl group (for MNZ) (Moore and Wilkins, 1990; Tong et al., 2011) and $C_{13}H_{12}N_2OF$ (for CIP) (Ferdig et al., 2005; Salma et al., 2016) are formed which are smaller than their parent ion (Fig. 8(b) (c)) and a faster degradation is observed. This reason is also satisfying for 100% degradation of MNZ and CIP in less time than other mixture antibiotics (Table 2).

Initially, the photodegradation process was rapid due to highly reactive radicals OH• which can oxidize MNZ, CIP and SMX.TiO$_2$ absorbs energy, they generate electrons (e^-) with high reducing ability and holes (h^+) with high oxidizing ability. These excited electrons(e^-) reduced O_2 hence generating superoxide radical ($^{\cdot}O_2^-$). While holes (h +) migrate to the surface of the photo-catalysts, H_2O will be oxidized to generate hydroxyl radical ($^{\cdot}OH$). MNZ, CIP and SMX could be decom-

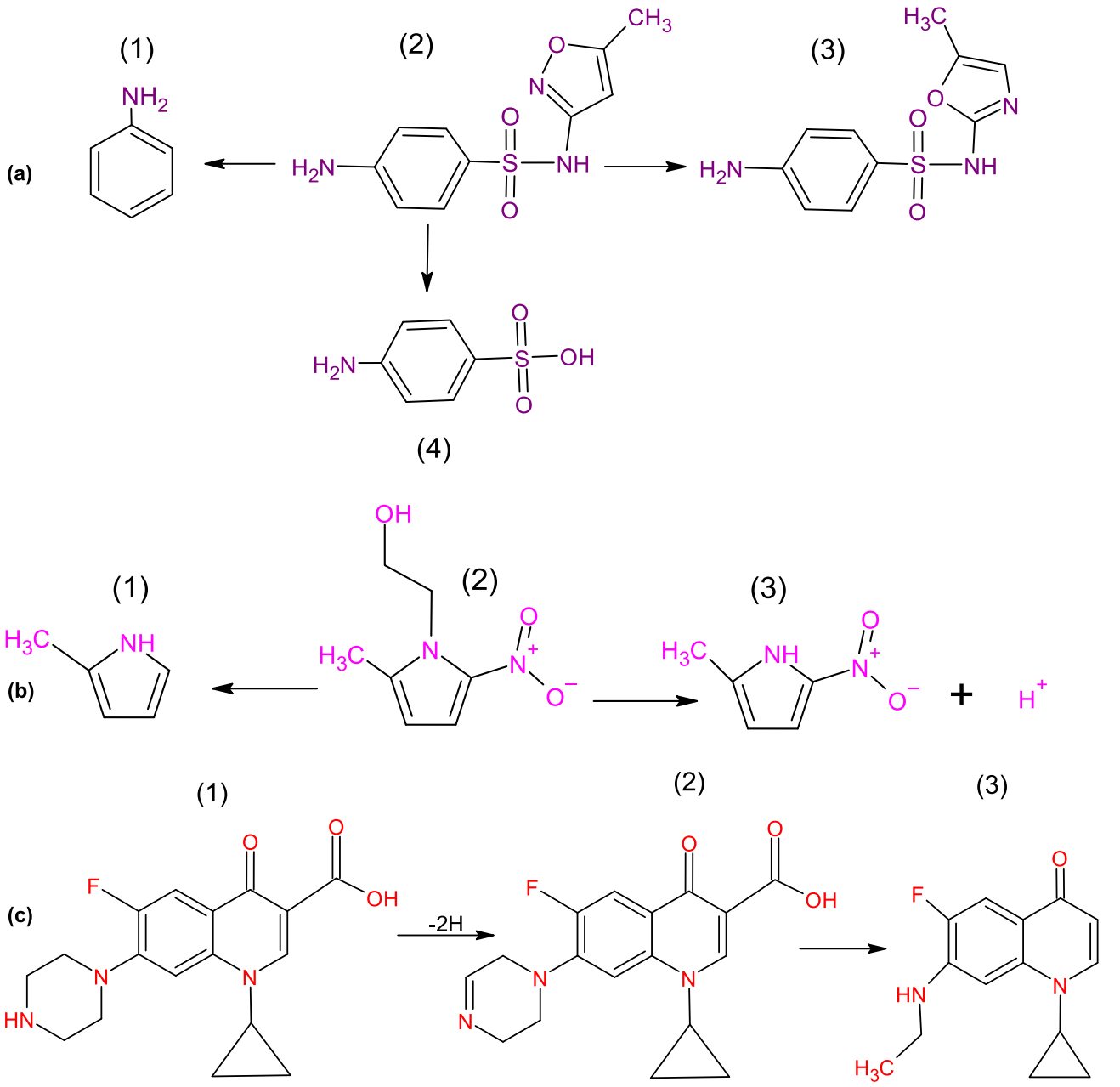

Fig. 8 Reaction scheme for photolysis of (a)SMX, (b)MNZ and (c)CIP.

posed by superoxide radical ($\cdot O_2^-$) or hydroxyl radical ($\cdot OH$). The mechanisms of photocatalytic oxidation are as following Eqs. (5)–(11) (Liu et al., 2018; Saadati et al., 2016).

$$TiO_2 + h\gamma \rightarrow TiO_2 + h^+ + e\text{-} \quad (2)$$

$$h^+ + OH^- \rightarrow \cdot OH \quad (3)$$

$$h^+ + H_2O + O_2 \rightarrow \cdot OH + H^+ + \cdot O_2^- \quad (4)$$

$$O_2 + e^- \rightarrow O_2^- \quad (5)$$

$$O_2^- + H^+ \rightarrow HO_2^- \quad (6)$$

$$2HO_2^- \rightarrow O_2 + H_2O_2 \quad (7)$$

$$H_2O_2 + \cdot O_2^- \rightarrow \cdot OH + OH^- + O_2 \quad (8)$$

Initially dissolved oxygen remains high in an aqueous solution. In other studies, it was found that initial dissolved oxygen was around 8 mg/L (Abellán et al., 2007), after the first hour of reaction it becomes 6 mg/L and is kept constant. Dissolved oxygen is highly electrophilic. It attracts electrons generated by the surface of TiO_2 (Eq. (2)) and reduced the undesirable electron-hole recombination. As initially more dissolved oxygen remains, more reactive radicals $OH^{\cdot}$ can produce to degrade antibiotics, that's why degradation occurs faster at the beginning. Lack of adsorption and the negligible photolysis, abatement of degradation occurs after 60 min, similar results found in previous literature (Mourid et al., 2020; Porcar-Santos et al., 2020). The influence of inorganic ions on the degradation of mixture antibiotics demands further studies.

3.5. Degradation pathways of SMX, MNZ and CIP

SMX (4-amino-N-(5 -methyl-3-isoxazolyl)benzenesulfonamide) photodegradation undergoes several reaction pathways. Before the total disappearance of SMX, many of the intermediate products (at least five primary photoproducts) were identified. The proposed reaction scheme (Luo et al., 2018; Zhou and Moore, 1994) is shown in Fig. 8(a). The major intermediate product is 4-amino-N-(5-methyl-2-oxazolyl)benzenesulfonamide (3) which is an isomer of SMX along with other products like sulfanilic acid (4) and aniline (1) (Zhou and Moore, 1994). Aniline and sulfanilic acid have also been identified as photo products from other sulfonamides. They are fromed from free radicals following homolytic γ-fission and δ-fission of sulfonamides (Chignell et al., 1980).

During photodegradation of metronidazole ($C_6H_9N_3O_3$) as shown in Fig. 12(b), metronidazole $C_6H_9N_3O_3$ (2) produces two unstable intermediates: the hydroxyethyl group (3) (m/z 128) and radical cation at m/z 82 (1) (Moore and Wilkins, 1990; Tong et al., 2011). Loss of hydroxyethyl group, metronidazole produces nitroimidazole and this ion is corresponded to the cleavage of the hydroxyethyl moiety (Tong et al., 2011). Elimination of nitro group from nitroimidazole to generate the radical cation.

During photodegradation as shown in Fig. 13(c), two photoproducts $C_{17}H_{16}N_3O_3F$ (2) and $C_{13}H_{12}N_2OF$ (3) were produced under photocatalytic oxidation (Ferdig et al., 2005; Salma et al., 2016). TiO_2 nanoparticles absorbed UV light (254 nm) which actuated to direct photo-hole (h +) oxidation and hydroxyl radical (An et al., 2010; Sturini et al., 2012) and interact with CIP ($C_{17}H_{18}N_3O_3F$) as mentioned in reaction mechanisms. It especially occurs in presence of TiO_2, at the piperazing ring with preservation of the fluorine.

4. Conclusion

SMX, MNZ and CIP were successfully removed from aqueous solution using UV/TiO_2 photodegradation technique at their inherent pH. 97% degradation of SMX was observed within 360 min for 5 mg/L SMX concentration which was 86% at 460 min for 80 mg/L SMX concentration. The optimum dosage of TiO_2 was 0.7 g/L for SMX degradation. MNZ and CIP removals were 100% and 89%, respectively, at 600 min of photodegradation reaction. 100% degradation was observed at 120 min for MNZ and CIP binary mixture, whereas the degradations were 97% and 96% for SMX and MNZ, and SMX and CIP binary mixtures, respectively, even after 600 min of experimental time at the same concentrations. For tertiary mixture, the maximum removal 99% was observed for ([SMX = CIP] = 20 mg/L and [MNZ] = [40 mg/L]) at 600 min of experimental time. For mixture, it has been observed that the degradation was faster for lower concentration of SMX. The results indicate that the commercial TiO_2 at low cost is promising under UV irradiation for the reclamation of pharmaceutical wastewaters.

CRediT authorship contribution statement

Surya Akter: Conceptualization, Data curation, Methodology, Validation, Writing – original draft. **Md. Sahinoor Islam:** Investigation, Methodology, Writing – review & editing. **Md. Humayun Kabir:** Formal analysis, Writing – review & editing. **Md. Aftab Ali Shaikh:** Project administration, Resources, Supervision. **Md. Abdul Gafur:** Project administration, Resources, Supervision, Conceptualization, Writing – review & editing.

Declaration of Competing Interest

The authors declare that they have no known competing financial interests or personal relationships that could have appeared to influence the work reported in this paper.

Acknowledgements

The authors acknowledge the authority of Bangladesh Council of Scientific and Industrial Research, Ministry of S&T, Bangladesh for providing funding and testing facilities.

Appendix A. Supplementary material

Supplementary data to this article can be found online at https://doi.org/10.1016/j.arabjc.2022.103900.

References

Abellán, M.N., Bayarri, B., Giménez, J., Costa, J., 2007. Photocatalytic degradation of sulfamethoxazole in aqueous suspension of TiO2. Appl. Catal. B Environ. 74, 233–241. https://doi.org/10.1016/j.apcatb.2007.02.017.

Ahmadi, E., Kakavandi, B., Azari, A., Izanloo, H., Gharibi, H., Mahvi, A.H., Javid, A., Hashemi, S.Y., 2016. The performance of mesoporous magnetite zeolite nanocomposite in removing dimethyl phthalate from aquatic environments. Desalination Water Treat. 1–15. https://doi.org/10.1080/19443994.2016.1178174.

Ahmed, O., Zahraa, O., 2014. Degradation of sulfamethoxazole by photocatalysis using supported TiO2 8.

Al-Mamun, M.R., Kader, S., Islam, M.S., 2021. Solar-TiO2 immobilized photocatalytic reactors performance assessment in the degradation of methyl orange dye in aqueous solution. Environ. Nanotechnol. Monit. Manag. 16, 100514. https://doi.org/10.1016/j.enmm.2021.100514.

An, T., Yang, H., Song, W., Li, G., Luo, H., Cooper, W.J., 2010. Mechanistic considerations for the advanced oxidation treatment of fluoroquinolone pharmaceutical compounds using TiO $_2$ heterogeneous catalysis. J. Phys. Chem. A 114, 2569–2575. https://doi.org/10.1021/jp911349y.

Angeles, L.F., Islam, S., Aldstadt, J., Saqeeb, K.N., Alam, M., Khan, M.A., Johura, F.-T., Ahmed, S.I., Aga, D.S., 2020. Retrospective suspect screening reveals previously ignored antibiotics, antifungal compounds, and metabolites in Bangladesh surface waters. Sci. Total Environ. 712,. https://doi.org/10.1016/j.scitotenv.2019.136285 136285.

Azari, A., Nabizadeh, R., Mahvi, A.H., Nasseri, S., 2021a. Magnetic multi-walled carbon nanotubes-loaded alginate for treatment of industrial dye manufacturing effluent: adsorption modelling and process optimisation by central composite face-central design. Int. J. Environ. Anal. Chem. 1–21. https://doi.org/10.1080/03067319.2021.1877279.

Azari, A., Nabizadeh, R., Mahvi, A.H., Nasseri, S., 2020. Integrated Fuzzy AHP-TOPSIS for selecting the best color removal process using carbon-based adsorbent materials: multi-criteria decision making vs. systematic review approaches and modeling of textile wastewater treatment in real conditions. Int. J. Environ. Anal. Chem. 1–16. https://doi.org/10.1080/03067319.2020.1828395.

Azari, A., Yeganeh, M., Gholami, M., Salari, M., 2021b. The superior adsorption capacity of 2,4-Dinitrophenol under ultrasound-assisted magnetic adsorption system: Modeling and process optimization by

central composite design. J. Hazard. Mater. 418,. https://doi.org/10.1016/j.jhazmat.2021.126348 126348.

Babuponnusami, A., Muthukumar, K., 2014. A review on Fenton and improvements to the Fenton process for wastewater treatment. J. Environ. Chem. Eng. 2, 557–572. https://doi.org/10.1016/j.jece.2013.10.011.

Bagnis, S., Boxall, A., Gachanja, A., Fitzsimons, M., Murigi, M., Snape, J., Tappin, A., Wilkinson, J., Comber, S., 2020. Characterization of the Nairobi River catchment impact zone and occurrence of pharmaceuticals: Implications for an impact zone inclusive environmental risk assessment. Sci. Total Environ. 703,. https://doi.org/10.1016/j.scitotenv.2019.134925 134925.

Carlsson, C., Johansson, A.-K., Alvan, G., Bergman, K., Kühler, T., 2006. Are pharmaceuticals potent environmental pollutants? Sci. Total Environ. 364, 67–87. https://doi.org/10.1016/j.scitotenv.2005.06.035.

Chen, G., Yu, Y., Liang, L., Duan, X., Li, R., Lu, X., Yan, B., Li, N., Wang, S., 2021. Remediation of antibiotic wastewater by coupled photocatalytic and persulfate oxidation system: A critical review. J. Hazard. Mater. 408,. https://doi.org/10.1016/j.jhazmat.2020.124461 124461.

Chignell, C.F., Kalyanaraman, B., Mason, R.P., Sik, R.H., 1980. Spectroscopic studies of cutaneous photosensitizing agents—I. Spin trapping of photolysis products from sulfanilamide, 4-aminobenzoic acid and related compounds. Photochem. Photobiol. 32, 563–571. https://doi.org/10.1111/j.1751-1097.1980.tb04023.x.

Crini, G., Lichtfouse, E., 2019. Advantages and disadvantages of techniques used for wastewater treatment. Environ. Chem. Lett. 17, 145–155. https://doi.org/10.1007/s10311-018-0785-9.

Dharwadkar, S., Yu, L., Achari, G., 2021. Enhancement of LED based photocatalytic degradation of sulfolane by integration with oxidants and nanomaterials. Chemosphere 263,. https://doi.org/10.1016/j.chemosphere.2020.128124 128124.

Evgenidou, E., Chatzisalata, Z., Tsevis, A., Bourikas, K., Torounidou, P., Sergelidis, D., Koltsakidou, A., Lambropoulou, D.A., 2021. Photocatalytic degradation of a mixture of eight antibiotics using Cu-modified TiO2 photocatalysts: Kinetics, mineralization, antimicrobial activity elimination and disinfection. J. Environ. Chem. Eng. 9,. https://doi.org/10.1016/j.jece.2021.105295 105295.

Farzadkia, M., Bazrafshan, E., Esrafili, A., Yang, J.-K., Shirzad-Siboni, M., 2015. Photocatalytic degradation of Metronidazole with illuminated TiO2 nanoparticles. J. Environ. Health Sci. Eng. 13, 35. https://doi.org/10.1186/s40201-015-0194-y.

Ferdig, M., Kaleta, A., Buchberger, W., 2005. Improved liquid chromatographic determination of nine currently used (fluoro) quinolones with fluorescence and mass spectrometric detection for environmental samples. J. Sep. Sci. 28, 1448–1456. https://doi.org/10.1002/jssc.200400065.

Gan, Y., Wei, Y., Xiong, J., Cheng, G., 2018. Impact of post-processing modes of precursor on adsorption and photocatalytic capability of mesoporous TiO2 nanocrystallite aggregates towards ciprofloxacin removal. Chem. Eng. J. 349, 1–16. https://doi.org/10.1016/j.cej.2018.05.051.

Garcia-Ivars, J., Martella, L., Massella, M., Carbonell-Alcaina, C., Alcaina-Miranda, M.-I., Iborra-Clar, M.-I., 2017. Nanofiltration as tertiary treatment method for removing trace pharmaceutically active compounds in wastewater from wastewater treatment plants. Water Res. 125, 360–373. https://doi.org/10.1016/j.watres.2017.08.070.

Grenni, P., Ancona, V., Barra Caracciolo, A., 2018. Ecological effects of antibiotics on natural ecosystems: A review. Microchem. J. 136, 25–39. https://doi.org/10.1016/j.microc.2017.02.006.

Gutierrez, A., Laureti, L., Crussard, S., Abida, H., Rodríguez-Rojas, A., Blázquez, J., Baharoglu, Z., Mazel, D., Darfeuille, F., Vogel, J., Matic, I., 2013. β-lactam antibiotics promote bacterial mutagenesis via an RpoS-mediated reduction in replication fidelity. Nat. Commun. 4, 1610. https://doi.org/10.1038/ncomms2607.

Hasan Khan Neon, M., Islam, M.S., 2019. MoO3 and Ag co-synthesized TiO2 as a novel heterogeneous photocatalyst with enhanced visible-light-driven photocatalytic activity for methyl orange dye degradation. Environ. Nanotechnol. Monit. Manag. 12, 100244. https://doi.org/10.1016/j.enmm.2019.100244.

Hossain, A., Nakamichi, S., Habibullah-Al-Mamun, M.d., Tani, K., Masunaga, S., Matsuda, H., 2018. Occurrence and ecological risk of pharmaceuticals in river surface water of Bangladesh. Environ. Res. 165, 258–266. https://doi.org/10.1016/j.envres.2018.04.030.

Hossain, A., Nakamichi, S., Habibullah-Al-Mamun, M.d., Tani, K., Masunaga, S., Matsuda, H., 2017. Occurrence, distribution, ecological and resistance risks of antibiotics in surface water of finfish and shellfish aquaculture in Bangladesh. Chemosphere 188, 329–336. https://doi.org/10.1016/j.chemosphere.2017.08.152.

Javid, N., Honarmandrad, Z., Malakootian, M., 2020. Ciprofloxacin removal from aqueous solutions by ozonation with calcium peroxide. Desalination Water Treat. 174, 178–185. https://doi.org/10.5004/dwt.2020.24855.

Kanakaraju, D., Glass, B.D., Oelgemöller, M., 2018. Advanced oxidation process-mediated removal of pharmaceuticals from water: A review. J. Environ. Manage. 219, 189–207. https://doi.org/10.1016/j.jenvman.2018.04.103.

Khan, N.A., Ahmed, S., Farooqi, I.H., Ali, I., Vambol, V., Changani, F., Yousefi, M., Vambol, S., Khan, S.U., Khan, A.H., 2020. Occurrence, sources and conventional treatment techniques for various antibiotics present in hospital wastewaters: A critical review. TrAC Trends Anal. Chem. 129,. https://doi.org/10.1016/j.trac.2020.115921 115921.

Kim, J.R., Kan, E., 2016. Heterogeneous photocatalytic degradation of sulfamethoxazole in water using a biochar-supported TiO2 photocatalyst. J. Environ. Manage. 180, 94–101. https://doi.org/10.1016/j.jenvman.2016.05.016.

Leung, H.W., Jin, L., Wei, S., Tsui, M.M.P., Zhou, B., Jiao, L., Cheung, P.C., Chun, Y.K., Murphy, M.B., Lam, P.K.S., 2013. Pharmaceuticals in tap water: human health risk assessment and proposed monitoring framework in China. Environ. Health Perspect. 121, 839–846. https://doi.org/10.1289/ehp.1206244.

Li, Y., Fu, Y., Zhu, M., 2020. Green synthesis of 3D tripyramid TiO2 architectures with assistance of aloe extracts for highly efficient photocatalytic degradation of antibiotic ciprofloxacin. Appl. Catal. B Environ. 260,. https://doi.org/10.1016/j.apcatb.2019.118149 118149.

Liu, Q., Shen, J., Yang, X., Zhang, T., Tang, H., 2018. 3D reduced graphene oxide aerogel-mediated Z-scheme photocatalytic system for highly efficient solar-driven water oxidation and removal of antibiotics. Appl. Catal. B Environ. 232, 562–573. https://doi.org/10.1016/j.apcatb.2018.03.100.

Luo, S., Wei, Z., Spinney, R., Zhang, Z., Dionysiou, D.D., Gao, L., Chai, L., Wang, D., Xiao, R., 2018. UV direct photolysis of sulfamethoxazole and ibuprofen: An experimental and modelling study. J. Hazard. Mater. 343, 132–139. https://doi.org/10.1016/j.jhazmat.2017.09.019.

Mahmoodi Meimand, M., Javid, N., Malakootian, M., 2019. Adsorption of sulfur dioxide on clinoptilolite/nano iron oxide and natural clinoptilolite. Health Scope In Press. https://doi.org/10.5812/jhealthscope.69158.

Malakootian, M., Ahmadian, M., 2019. Ciprofloxacin removal by electro-activated persulfate in aqueous solution using iron electrodes. Appl. Water Sci. 9, 140. https://doi.org/10.1007/s13201-019-1024-7.

Malakootian, M., Kannan, K., Gharaghani, M.A., Dehdarirad, A., Nasiri, A., Shahamat, Y.D., Mahdizadeh, H., 2019. Removal of metronidazole from wastewater by Fe/charcoal micro electrolysis fluidized bed reactor. J. Environ. Chem. Eng. 7,. https://doi.org/10.1016/j.jece.2019.103457 103457.

Malakootian, M., Khatami, M., Mahdizadeh, H., Nasiri, A., Amiri Gharaghani, M., 2020a. A study on the photocatalytic degradation of *p* -Nitroaniline on glass plates by Thermo-Immobilized ZnO

nanoparticle. Inorg. Nano-Met. Chem. 50, 124–135. https://doi.org/10.1080/24701556.2019.1662807.

Malakootian, M., Nasiri, A., Amiri Gharaghani, M., 2020c. Photocatalytic degradation of ciprofloxacin antibiotic by TiO_2 nanoparticles immobilized on a glass plate. Chem. Eng. Commun. 207, 56–72. https://doi.org/10.1080/00986445.2019.1573168.

Malakootian, M., Shahesmaeili, A., Faraji, M., Amiri, H., Silva Martinez, S., 2020d. Advanced oxidation processes for the removal of organophosphorus pesticides in aqueous matrices: A systematic review and meta-analysis. Process Saf. Environ. Prot. 134, 292–307. https://doi.org/10.1016/j.psep.2019.12.004.

Martini, J., Orge, C.A., Faria, J.L., Pereira, M.F.R., Soares, O.S.G.P., 2018. Sulfamethoxazole degradation by combination of advanced oxidation processes. J. Environ. Chem. Eng. 6, 4054–4060. https://doi.org/10.1016/j.jece.2018.05.047.

Mohammed, A.A., Al-Musawi, T.J., Kareem, S.L., Zarrabi, M., Al-Ma'abreh, A.M., 2020. Simultaneous adsorption of tetracycline, amoxicillin, and ciprofloxacin by pistachio shell powder coated with zinc oxide nanoparticles. Arab. J. Chem. 13, 4629–4643. https://doi.org/10.1016/j.arabjc.2019.10.010.

Moore, D.E., Wilkins, B.J., 1990. Common products from gamma-radiolysis and ultraviolet photolysis of metronidazole. Int. J. Radiat. Appl. Instrum. Part C Radiat. Phys. Chem. 36, 547–550. https://doi.org/10.1016/1359-0197(90)90205-V.

Mourid, E.H., El Mouchtari, E.M., El Mersly, L., Benaziz, L., Rafqah, S., Lakraimi, M., 2020. Development of a new recyclable nanocomoposite LDH-TiO2 for the degradation of antibiotic sulfamethoxazole under UVA radiation: An approach towards sunlight. J. Photochem. Photobiol. Chem. 396,. https://doi.org/10.1016/j.jphotochem.2020.112530 112530.

Neghi, N., Kumar, M., 2017. Performance Analysis of Photolytic, Photocatalytic, and Adsorption Systems in the Degradation of Metronidazole on the Perspective of Removal Rate and Energy Consumption. Water. Air. Soil Pollut. 228, 339. https://doi.org/10.1007/s11270-017-3532-0.

Neghi, N., Kumar, M., Burkhalov, D., 2019. Synthesis and application of stable, reusable TiO2 polymeric composites for photocatalytic removal of metronidazole: Removal kinetics and density functional analysis. Chem. Eng. J. 359, 963–975. https://doi.org/10.1016/j.cej.2018.11.090.

Pereira, J.H.O.S., Reis, A.C., Queirós, D., Nunes, O.C., Borges, M.T., Vilar, V.J.P., Boaventura, R.A.R., 2013. Insights into solar TiO2-assisted photocatalytic oxidation of two antibiotics employed in aquatic animal production, oxolinic acid and oxytetracycline. Sci. Total Environ. 463–464, 274–283. https://doi.org/10.1016/j.scitotenv.2013.05.098.

Perini, J.A.L., Tonetti, A.L., Vidal, C., Montagner, C.C., Nogueira, R.F.P., 2018. Simultaneous degradation of ciprofloxacin, amoxicillin, sulfathiazole and sulfamethazine, and disinfection of hospital effluent after biological treatment via photo-Fenton process under ultraviolet germicidal irradiation. Appl. Catal. B Environ. 224, 761–771. https://doi.org/10.1016/j.apcatb.2017.11.021.

Porcar-Santos, O., Cruz-Alcalde, A., López-Vinent, N., Zanganas, D., Sans, C., 2020. Photocatalytic degradation of sulfamethoxazole using TiO2 in simulated seawater: Evidence for direct formation of reactive halogen species and halogenated by-products. Sci. Total Environ. 736,. https://doi.org/10.1016/j.scitotenv.2020.139605 139605.

Saadati, F., Keramati, N., Ghazi, M.M., 2016. Influence of parameters on the photocatalytic degradation of tetracycline in wastewater: A review. Crit. Rev. Environ. Sci. Technol. 46, 757–782. https://doi.org/10.1080/10643389.2016.1159093.

Salma, A., Thoröe-Boveleth, S., Schmidt, T.C., Tuerk, J., 2016. Dependence of transformation product formation on pH during photolytic and photocatalytic degradation of ciprofloxacin. J. Hazard. Mater. 313, 49–59. https://doi.org/10.1016/j.jhazmat.2016.03.010.

Shuchi, S.B., Suhan, M.B.K., Humayun, S.B., Haque, M.E., Islam, M.S., 2021. Heat-activated potassium persulfate treatment of Sudan Black B dye: Degradation kinetic and thermodynamic studies. J. Water Process Eng. 39,. https://doi.org/10.1016/j.jwpe.2020.101690 101690.

Silva, A.R., Martins, P.M., Teixeira, S., Carabineiro, S.A.C., Kuehn, K., Cuniberti, G., Alves, M.M., Lanceros-Mendez, S., Pereira, L., 2016. Ciprofloxacin wastewater treated by UVA photocatalysis: contribution of irradiated TiO_2 and ZnO nanoparticles on the final toxicity as assessed by Vibrio fischeri. RSC Adv 6, 95494–95503. https://doi.org/10.1039/C6RA19202E.

Sturini, M., Speltini, A., Maraschi, F., Profumo, A., Pretali, L., Irastorza, E.A., Fasani, E., Albini, A., 2012. Photolytic and photocatalytic degradation of fluoroquinolones in untreated river water under natural sunlight. Appl. Catal. B Environ. 119–120, 32–39. https://doi.org/10.1016/j.apcatb.2012.02.008.

Tong, L., Pérez, S., Gonçalves, C., Alpendurada, F., Wang, Y., Barceló, D., 2011. Kinetic and mechanistic studies of the photolysis of metronidazole in simulated aqueous environmental matrices using a mass spectrometric approach. Anal. Bioanal. Chem. 399, 421–428. https://doi.org/10.1007/s00216-010-4320-5.

Tran, M.L., Fu, C.-C., Juang, R.-S., 2019. Removal of metronidazole and amoxicillin mixtures by UV/TiO2 photocatalysis: an insight into degradation pathways and performance improvement. Environ. Sci. Pollut. Res. 26, 11846–11855. https://doi.org/10.1007/s11356-019-04683-4.

Triquet, T., Tendero, C., Latapie, L., Manero, M.-H., Richard, R., Andriantsiferana, C., 2020. TiO2 MOCVD coating for photocatalytic degradation of ciprofloxacin using 365 nm UV LEDs - kinetics and mechanisms. J. Environ. Chem. Eng. 8,. https://doi.org/10.1016/j.jece.2020.104544 104544.

Van der Bruggen, B., Mänttäri, M., Nyström, M., 2008. Drawbacks of applying nanofiltration and how to avoid them: A review. Sep. Purif. Technol. 63, 251–263. https://doi.org/10.1016/j.seppur.2008.05.010.

Verlicchi, P., Galletti, A., Petrovic, M., Barceló, D., 2010. Hospital effluents as a source of emerging pollutants: An overview of micropollutants and sustainable treatment options. J. Hydrol. 389, 416–428. https://doi.org/10.1016/j.jhydrol.2010.06.005.

Wang, H., Zhang, G., Gao, Y., 2010. Photocatalytic degradation of metronidazole in aqueous solution by niobate K6Nb10.8O30. Wuhan Univ. J. Nat. Sci. 15, 345–349. https://doi.org/10.1007/s11859-010-0664-0.

Wang, J., Wang, Z.G., Jin, X.D., Guo, Y.W., Gao, J.Q., Li, K., Wang, B.X., Li, Y., 2012. Catalytic damage of bovine serum albumin by metronidazole under ultrasonic irradiation in the presence of nano-sized TiO2 powder. Russ. J. Phys. Chem. A 86, 867–874. https://doi.org/10.1134/S0036024412050366.

Wang, J., Zhuan, R., 2020. Degradation of antibiotics by advanced oxidation processes: An overview. Sci. Total Environ. 701,. https://doi.org/10.1016/j.scitotenv.2019.135023 135023.

Wu, S., Liu, H., Lin, Y., Yang, C., Lou, W., Sun, J., Du, C., Zhang, D., Nie, L., Yin, K., Zhong, Y., 2020. Insights into mechanisms of UV/ferrate oxidation for degradation of phenolic pollutants: Role of superoxide radicals. Chemosphere 244,. https://doi.org/10.1016/j.chemosphere.2019.125490 125490.

Xekoukoulotakis, N.P., Drosou, C., Brebou, C., Chatzisymeon, E., Hapeshi, E., Fatta-Kassinos, D., Mantzavinos, D., 2011. Kinetics of UV-A/TiO2 photocatalytic degradation and mineralization of the antibiotic sulfamethoxazole in aqueous matrices. Catal. Today 161, 163–168. https://doi.org/10.1016/j.cattod.2010.09.027.

Xu, P., Janex, M.-L., Savoye, P., Cockx, A., Lazarova, V., 2002. Wastewater disinfection by ozone: main parameters for process design. Water Res. 36, 1043–1055. https://doi.org/10.1016/S0043-1354(01)00298-6.

Yousefzadeh, S., Ahmadi, E., Gholami, M., Ghaffari, H.R., Azari, A., Ansari, M., Miri, M., Sharafi, K., Rezaei, S., 2017. A comparative study of anaerobic fixed film baffled reactor and up-flow anaerobic

fixed film fixed bed reactor for biological removal of diethyl phthalate from wastewater: a performance, kinetic, biogas, and metabolic pathway study. Biotechnol. Biofuels 10, 139. https://doi.org/10.1186/s13068-017-0826-9.

Zhang, H., Wang, Z., Li, R., Guo, J., Li, Y., Zhu, J., Xie, X., 2017. TiO2 supported on reed straw biochar as an adsorptive and photocatalytic composite for the efficient degradation of sulfamethoxazole in aqueous matrices. Chemosphere 185, 351–360. https://doi.org/10.1016/j.chemosphere.2017.07.025.

Zheng, X., Xu, S., Wang, Y., Sun, X., Gao, Y., Gao, B., 2018. Enhanced degradation of ciprofloxacin by graphitized mesoporous carbon (GMC)-TiO2 nanocomposite: Strong synergy of adsorption-photocatalysis and antibiotics degradation mechanism. J. Colloid Interface Sci. 527, 202–213. https://doi.org/10.1016/j.jcis.2018.05.054.

Zhou, W., Moore, D.E., 1994. Photochemical decomposition of sulfamethoxazole. Int. J. Pharm. 110, 55–63. https://doi.org/10.1016/0378-5173(94)90375-1.